



# Beyond the Beta Rebound: Post-Task Responses in Oscillatory Activity follow Cessation of Working Memory Processes

Sebastian C. Coleman<sup>a</sup>, Zelekha A. Seedat<sup>a,b</sup>, Anna C. Whittaker<sup>c</sup>, Agatha Lenartowicz<sup>d</sup>, Karen J. Mullinger<sup>a,e,\*</sup>

<sup>a</sup> Sir Peter Mansfield Imaging Centre, School of Physics and Astronomy, University of Nottingham, Nottingham, NG7 2RD, UK

<sup>b</sup> Young Epilepsy, St Pier's Lane, Dormansland, Lingfield, RH7 6PW, UK

<sup>c</sup> Faculty of Health Sciences and Sport, University of Stirling, Stirling, UK

<sup>d</sup> Department of Psychiatry & Biobehavioral Sciences, University of California Los Angeles

<sup>e</sup> Centre for Human Brain Health, School of Psychology, University of Birmingham, UK

## ARTICLE INFO

### Key words:

Magnetoencephalography  
neural oscillations  
post-stimulus rebound  
post-stimulus response  
event-related synchronisation  
event-related desynchronisation  
n-back

## ABSTRACT

Post-task responses (PTRs) are transitional responses occurring for several seconds between the end of a stimulus/task and a period of rest. The most well-studied of these are beta band (13 – 30 Hz) PTRs in motor networks following movement, often called post-movement beta rebounds, which have been shown to differ in patients with schizophrenia and autism. Previous studies have proposed that beta PTRs reflect inhibition of task-positive networks to enable a return to resting brain activity, scaling with cognitive demand and reflecting cortical self-regulation. It is unknown whether PTRs are a phenomenon of the motor system, or whether they are a more general self-modulatory property of cortex that occur following cessation of higher cognitive processes as well as movement. To test this, we recorded magnetoencephalography (MEG) responses in 20 healthy participants to a working-memory task, known to recruit cortical networks associated with higher cognition. Our results revealed PTRs in the theta, alpha and beta bands across many regions of the brain, including the dorsal attention network (DAN) and lateral visual regions. These PTRs increased significantly ( $p < 0.05$ ) in magnitude with working-memory load, an effect which is independent of oscillatory modulations occurring over the task period as well as those following individual stimuli. Furthermore, we showed that PTRs are functionally related to reaction times in left lateral visual ( $p < 0.05$ ) and left parietal ( $p < 0.1$ ) regions, while the oscillatory responses measured during the task period are not. Importantly, motor PTRs following button presses did not modulate with task condition, suggesting that PTRs in different networks are driven by different aspects of cognition. Our findings show that PTRs are not limited to motor networks but are widespread in regions which are recruited during the task. We provide evidence that PTRs have unique properties, scaling with cognitive load and correlating significantly with behaviour. Based on the evidence, we suggest that PTRs inhibit task-positive network activity to enable a transition to rest, however, further investigation is required to uncover their role in neuroscience and pathology.

## 1. Introduction

Post-task responses (PTRs) occur in a transition period, starting when a stimulus or task has ended, lasting for up to ten seconds before the brain returns to resting state and the associated oscillatory rhythms. PTRs have previously been termed post-stimulus responses or rebounds, primarily due to them being studied in response to simple sensorimotor

stimuli rather than higher cognitive tasks. They are commonly reported in electrophysiological recordings using electroencephalography (EEG) and magnetoencephalography (MEG), primarily in the motor cortex (Fry et al. 2016; Pakenham et al. 2020; Robson et al. 2016). In addition, haemodynamic PTRs are documented in studies using functional magnetic resonance imaging (fMRI) (Frahm et al. 1996) and observed over a variety of brain regions (Gonzalez-Castillo et al. 2012;

*List of abbreviations:* MEG, Magnetoencephalography; PTR, Post Task Response; OTR, Oscillatory Task Response; OSR, Oscillatory Stimulus Response; PMBR, Post Movement Beta Rebound; MRBD, Movement Related Beta Decrease; ERS/ERD, Event Related Synchronisation/Desynchronisation; WM, Working Memory; RT, Reaction Times; TH, Targets Hit; FP, False Presses; rm-ANOVA, Repeated Measures Analysis of Variance; T-stat, Pseudo T-statistic; VE, Virtual Electrode; TPJ, Temporoparietal Junction; DAN, Dorsal Attention Network; DMN, Default Mode Network; TFS, Time Frequency Spectrogram; SLR, Simple Linear Regression.

\* Address for Correspondence: Karen Mullinger, Sir Peter Mansfield Imaging Centre, School of Physics and Astronomy, University of Nottingham, Nottingham, NG7 2RD, UK

E-mail address: [karen.mullinger@nottingham.ac.uk](mailto:karen.mullinger@nottingham.ac.uk) (K.J. Mullinger).

<https://doi.org/10.1016/j.neuroimage.2022.119801>.

Received 23 September 2022; Received in revised form 23 November 2022; Accepted 5 December 2022

Available online 8 December 2022.

1053-8119/© 2022 Published by Elsevier Inc. This is an open access article under the CC BY-NC-ND license (<http://creativecommons.org/licenses/by-nc-nd/4.0/>)

Hanlon *et al.* 2016; Yamamoto *et al.* 2014). The origin of the haemodynamic PTR, neuronal or vascular, remains an area of active research due to the complexity of the blood oxygenation level dependant (BOLD) signal (van Zijl *et al.* 2012; Uludag and Blinder 2018). Current knowledge is lacking with regards to the prevalence of electrophysiological PTRs across the whole brain and the functional role they play. This work focuses on electrophysiological PTRs across all frequency bands as a direct, and potentially unique, measure of neuronal activity.

The beta band (13 – 30 Hz) PTR in the motor cortex, often termed the post-movement beta rebound (PMBR), is the most well-studied electrophysiological PTR. The PMBR is characterised by a rise in beta band power above baseline following cessation of movement, driven by increased probability of beta bursting events (Pfurtscheller 1981; Pfurtscheller and Lopes da Silva 1999). These are induced, rather than evoked, effects and are currently *not* thought to be related to other well documented evoked responses such as error-related negativity (ERN) (Falkenstein *et al.* 1991; Gehring *et al.* 1995; Gehring *et al.* 2018) or contingent negative variation (CNV) (Walter 1968; Babiloni *et al.* 2005), although explicit relationships are yet to be investigated. The PMBR modulates with various task parameters, e.g., increases with force output (Fry *et al.* 2016) and decreases with movement duration (Pakenham *et al.* 2020). The PMBR has also been shown to differ in several patient populations compared to healthy controls (Gascoyne *et al.* 2021; Liddle *et al.* 2016; Robson *et al.* 2016; Gaetz *et al.* 2020). The response preceding the PMBR, termed the movement-related beta decrease (MRBD), remained unchanged during these experiments. Together, these studies showed that the PMBR is modulated independently of the MRBD and can be predictive of symptoms related to disease severity in a way that the MRBD is not. In turn, this suggests that the PMBR is a window into a period of unique brain activity. The neural mechanisms underlying the PMBR remain unknown, but it has been posited that the PMBR is required to actively inhibit the motor network to prevent further movement from taking place (Chen *et al.* 1999; Pakenham *et al.* 2020). Pakenham *et al.* suggested that task difficulty drives PMBR amplitude, such that greater cognitive load in the motor network requires greater levels of inhibition (thus larger PMBR) when returning to rest. The direct relationship between difficulty and the PMBR was not tested directly as there were no differences in behavioural measures of task difficulty that could be related to PMBR amplitude. Another hypothesis is that the PMBR is a marker of certainty in the brain's feed-forward model related to the task, such that greater uncertainty in the motor action leads to diminished PMBRs (Tan *et al.* 2014). The two studies above cannot be directly compared, as the study by Pakenham *et al.* varied the duration of grip force, which changed the difficulty of the motor action, whereas the study by Tan *et al.* varied the degree of mismatch between the internal motor plan and the outcome of the motion, thus modulating motor uncertainty rather than difficulty of execution.

Outside of the motor system, relatively few reports of PTRs have been documented. Alpha band (8 – 13 Hz) PTRs have been reported in the visual cortex (Mullinger *et al.* 2017), although these are poorly studied. To our knowledge, there have been no reported electrophysiological PTRs outside of the primary cortex (i.e., outside of primary motor, somatosensory, visual or auditory cortices). Liddle *et al.* reported a “post-stimulus response” in the insula following task-relevant stimuli (Liddle *et al.* 2016). However, this response began whilst the visual stimulus was presented and took place in a period of active memory maintenance, i.e., not before the brain returns to rest as per our definition of a PTR. Thus, it is unclear whether the response reported by Liddle *et al.* is a true PTR or an oscillatory response generated for memory maintenance (Jensen *et al.* 2002; Tuladhar *et al.* 2007). It is currently unknown whether PTRs are unique to the primary cortex and basic sensory processing, or whether they are also elicited in higher order areas following complex cognitive processes. The distinction is important as it determines whether PTRs are a functional property of primary cortical regions, or a ubiquitous self-modulatory property of the entire cortex.

To study PTRs following higher cognitive processes we employ an n-back task that: i) recruits brain regions associated with higher cognitive activity; ii) maintains a relatively constant load in the recruited brain regions during task periods so that the task has definitive on/off periods; iii) modulates cognitive load between task conditions without changing sensory input. Crucially, our n-back task contained long (30 s) rest periods after each task period, allowing for the study of PTRs. We hypothesise that PTRs occur in higher cognitive regions and provide unique information about cognitive processing which is not obtained from the oscillatory task-response (OTR, average MEG response measured *during* the task period). Furthermore, we aim to corroborate the previously posed hypothesis (Pakenham *et al.* 2020) that PTRs are driven by perceived task difficulty by relating PTR amplitude to behavioural measures of task performance. This will provide vital new information as to the functional importance of PTRs.

## 2. Materials and Methods

### 2.1. Subjects

20 healthy volunteers (10 female, aged  $26 \pm 4$  [mean  $\pm$  SD] years) took part in this study, which was approved by the University of Nottingham Medical School Research Ethics Committee and in compliance with all COVID-19 standard operating procedures. All volunteers gave written, informed consent.

### 2.2. Paradigm

A summary of the n-back paradigm used in the experiment is shown in Fig. 1. The n-back task conditions were 0-back, 1-back and 2-back (Fig. 1C), in order of increasing working memory (WM) load. Subjects were instructed to use their right index finger to press a button when a target letter was shown. Depending on the block condition, the target letter was either the letter ‘x’ (0-back), the same letter as the letter before (1-back), or the same letter as two letters before (2-back). At the start of each block, an instruction screen was presented for 2 s which displayed the forthcoming task condition. During a task period, 15 letters (which we term stimuli), 4 of which were targets, were presented for 1 s each in a pseudorandom order, with 1 s of blank screen between sequential letters. Each task period was followed by a 30 s rest period, during which a fixation dot was shown. The instruction screen, task period, and rest period formed an experimental block lasting 62 s. The experiment comprised of 2 runs with 8 blocks per condition in each run. Blocks were arranged in a different pseudorandom order for each of the runs. The oscillatory task response (OTR) window was defined as 0.5 – 29.5 s, and encompasses slow induced oscillatory changes that span the entire task window, while the post-task response (PTR) window was defined as 31.5 – 33.5 s, positioned at the peak of post-task induced oscillatory changes. The oscillatory stimulus response (OSR) window was defined as 0.3 – 0.5 s following the start of each stimulus presentation, positioned around the peak of fast induced changes that occur following each new WM item.

### 2.3. Data Acquisition

Data were collected at a sampling rate of 600 Hz using a 275-channel CTF MEG system (MISL, Coquitlam, BC, Canada) in third order gradiometer configuration. Head localisation coils were attached to the subjects' nasion and preauricular points prior to scanning to provide fiducial markers for head localisation. The coils were energised before the start and after the end of each run to provide a measure of overall head movement. The subjects were scanned in a seated position in front of a projector screen approximately 80 cm away that displayed the stimuli for the experiment. An eye-tracker (EyeLink, Ottawa, Canada) was used to monitor the subjects to ensure they remained awake during the relatively long rest periods.

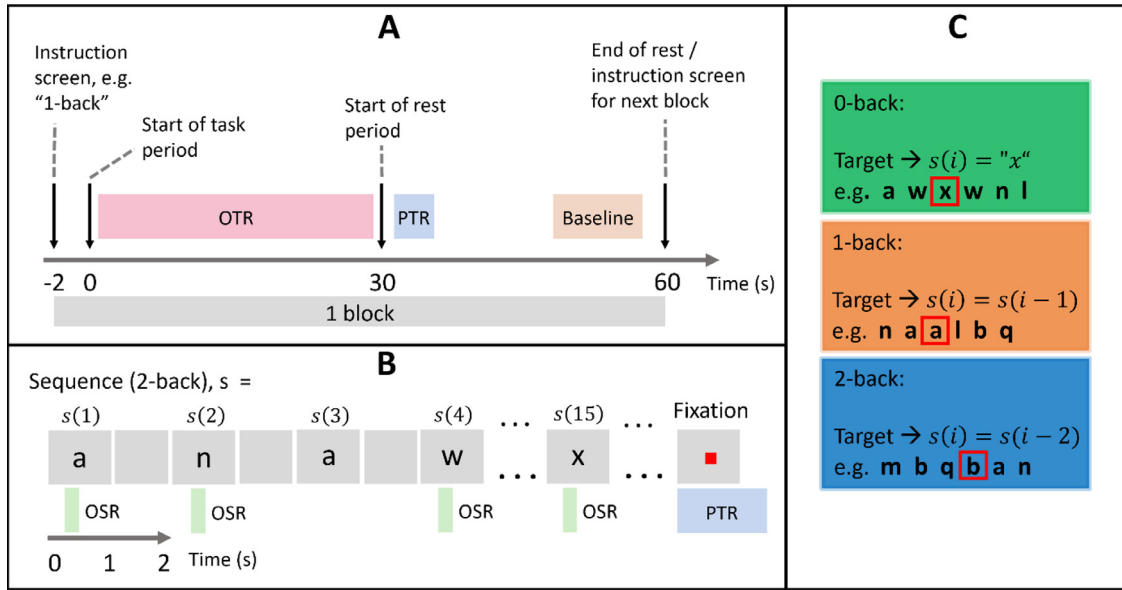


**Fig. 1.** The n-back paradigm.

Panel A: Each block started with an instruction screen at -2 s, which read either "0-back", "1-back" or "2-back", indicating the condition that would follow. The task period started at 0 s, lasting for 30 s. The rest period started at 30 s and lasted for 30 s. At 60 s, the instruction screen for the next block was shown. The oscillatory task response (OTR) window (0.5 - 29.5 s), the post-task response (PTR) window (31.5 - 33.5 s) and the baseline window (48 - 58 s) are shown. Panel B shows the timing of the presentation of individual stimuli and indicates oscillatory stimulus response (OSR) window (0.3 - 0.5 s following the start of each stimulus presentation). Panel C shows the three different task conditions, with the red boxes indicating the target letters. Each subject completed a total of 16 blocks of each condition, in a pseudorandom order, spread over two separate runs.

In between the two runs, a 3D digital mesh of the head and fiducial coils was acquired using a structure sensor (Occipital, Colorado, USA). Before the head digitisation, subjects were fitted with a swimming cap to flatten down hair, and green stickers were placed on the fiducial coils to enable easy identification of these locations on the head. The digitised head surface and fiducial locations were then co-registered with an anatomical MRI ( $T_1$ -weighted MPRAGE sequence acquired on either a 3T or 7T MRI scanner) to allow the position of the sensors relative to the brain to be determined.

## 2.4. Data Analysis

### 2.4.1. Behavioural metrics

Button press responses were used to calculate three primary behavioural metrics relating to n-back task performance: targets hit (TH), false presses (FP) and reaction times (RT). Both TH and FP were calculated using an acceptance threshold of 1.8 s, i.e., a correct button press must have occurred within 1.8 s of the start of presentation of the target, and similarly, a false press must have occurred within 1.8 s of a non-target being presented. RT were only measured for correct button presses. These measures were averaged across runs and subjects to give an overall measure for each condition. The significance of modulations between conditions of each behavioural measure were found using repeated-measures analysis of variance (rm-ANOVA) tests.

### 2.4.2. MEG Pre-processing

The sensor-level MEG data were bandpass filtered into 1-150 Hz and DC offset was removed. Data were segmented into blocks and grouped by task condition. Eye-tracker data were visually inspected to ascertain whether subjects had stayed awake. Each 62 s block was visually inspected and any that contained sensor resets or movement were removed. After removal of noisy data, an average of  $46 \pm 1$  blocks per subject remained across all conditions to be used for all further analysis. Eye-blink and cardiac artifacts were then removed from the remaining data using ICA in Fieldtrip (<https://www.fieldtriptoolbox.org/>). All 20 subject datasets remained for further analysis after the pre-processing.

### 2.4.3. Activation Maps and Timecourses

A linearly-constrained minimum-variance beamformer was applied to the entire subject dataset to transform the sensor-level data into source-space, with 4 mm cubic voxels, using the covariance of the entire subject dataset. Two separate contrasts were used to calculate pseudo T-statistic (F-stat) maps of the OTR and PTR modulations to the task. The F-stat maps were created using the following time-windows: i) the OTR window (0.5 - 29.5 s); ii) the PTR window, (31.5 - 33.5 s), when the PTR was expected to be the largest. For each of these time windows the 2-back condition was contrasted against the 0-back condition to identify the regions which were most strongly modulated by condition. This contrast was preferable over contrasting each time window with a section of the rest period as it was invariant to baseline drifting – this was especially important with the PTR F-stat maps as the PTR window only lasted 2 s, and would therefore be very sensitive to the 2 s contrast window within the rest period that was chosen. To identify PTR activity which may occur in different frequency bands, F-stat maps were calculated for the following: theta (4 - 8 Hz), alpha (8 - 13 Hz), beta (13 - 30 Hz), low gamma (30 - 50 Hz) and high gamma (50 - 100 Hz) bands. For completeness, additional analysis to create F-stat maps by contrasting the OTR time window (0.5 - 29.5 s) with a conventional rest window (30.5 - 59.5 s) [which encompasses the PTR period] was performed, akin to previous studies (Brookes et al. 2011; Luckhoo et al. 2012) (see Supplementary Information).

The F-stat maps for each subject and frequency band were moved into the standard MNI space using the MNI 152 brain template, allowing maps to be averaged to create a set of group F-stat maps. The anatomical masks (Table 1) were transformed into individual subject-space and applied to the original F-stat maps for each subject. The peak (maxima or minima) F-stat within each masked region was found for each subject to become the virtual electrode (VE) location, representing the location of maximal event-related synchronisation/desynchronisation (ERS/ERD), respectively. Broadband (1 - 150 Hz) VE timecourses were extracted from these VE locations. The timecourses from each VE were then used to create time-frequency spectrograms (TFS) to identify whether responses at a given location were broadband or frequency band specific.

**Table 1**  
Anatomical masks.

Mask Name	OTR/PTR Window	Band(s)	Source/Ref
Frontal	OTR, PTR	Theta	Combined AAL regions
Left Parietal	OTR, PTR	Alpha, Beta	Combined AAL regions
Right Parietal	OTR	Alpha, Beta	Combined AAL regions
Left Lateral Visual	OTR, PTR	Alpha	(Przedzik et al. 2013; Wilson et al. 2015)
Right Lateral Visual	OTR	Alpha	(Przedzik et al. 2013; Wilson et al. 2015)
Left Frontal Eye Field	PTR	Beta	(Przedzik et al. 2013; Wilson et al. 2015)
Right TPJ	PTR	Theta	(Mars et al. 2012)
Left Sensorimotor	PTR	Theta	(Przedzik et al. 2013; Wilson et al. 2015)

Masks used to interrogate the strongest responses during the OTR window (0.5 - 29.5 s) and PTR window (31.5 - 33.5 s).

The TFS were made by taking the power envelope of bandpass filtered data for a range of frequency limits (2 - 4 Hz, 4 - 8 Hz, 8 - 12 Hz, 12 - 16 Hz, 16 - 20 Hz, 20 - 24 Hz, 24 - 28 Hz, 28 - 32 Hz), before averaging over blocks for each frequency so that the time evolution of average spectral data over a block period could be plotted. Then, using the same frequency limits as the corresponding T-stat maps, the data from each location were bandpass filtered, Hilbert transformed and the resultant power envelopes were averaged over blocks to produce block-averaged timecourses for each subject and condition. Baselines were removed (usually referred to as baseline-correction) from the TFS and timecourses using the time-window of 48 - 58 s (see Fig. 1A) and averaged across subjects to reveal group-level effects for each frequency band and location.

To reveal statistical differences between conditions, time-averaged oscillatory power was calculated for each subject during the relevant time-window for each response (e.g. the timecourses at locations/frequencies with maximal PTR activity were averaged across the time-window of the PTR and similarly for OTRs). Each of these average responses were tested for significant modulations between conditions using rm-ANOVA. Bonferroni correction was used to adjust p-values for multiple comparisons. In regions where a significant effect of condition was observed after Bonferroni correction, post-hoc t-tests were used to establish which condition(s) were driving the measured effects.

To test whether the PTR modulations between conditions in a given frequency band were independent from the changes in OTR we performed a regression analysis. For regions and frequency bands where a response was observed in both time windows (see Table 1), individual subject OTR and PTR measures were taken for each block. A simple linear regression (SLR) between these measures for a given region and frequency band was then performed, and the trend between OTR and PTR amplitude was removed from the PTR amplitude to create the residual PTR amplitude for each block. The average residual PTR was calculated over blocks for each condition, and rm-ANOVAs were performed across conditions over the group to determine whether modulations were significant, again corrected for multiple comparisons.

To compare PTRs following higher cognition with the well-studied PMBR, the beta response following successful button presses was analysed. The VE location was taken from a T-stat map that contrasted the PMBR window (0.5 - 1.5 s following each button press) with the MRBD window (-0.5 - 0.5 s around each button press), which was then used to plot the peak beta band timecourse with an epoch of -1 - 2 s around the button press. The MRBD and PMBR windows were both tested for significant modulation with task condition using rm-ANOVA.

Additional analyses were performed to investigate the relationship between PTRs and the oscillatory stimulus response (OSR, oscillatory response following each letter presentation), see Fig. 1B and Supplementary Information.

#### 2.4.4. Neural-Behaviour Correlations

To test our hypothesis that PTRs are related to behavioural measures of task difficulty we related the PTRs to RT. For both the behavioural and oscillatory measures, the difference between 2-back and 1-back was

calculated per subject. SLRs were then performed to find the correlation and corresponding p values between RT and oscillatory response in regions containing a peak in both the OTR and PTR period T-stat maps. The difference between 2-back and 1-back was chosen as there was much greater variability in the RT of subjects performing the 0-back condition than 1-back condition. The reason for this may have been waning concentration due to the simplicity of the 0-back condition. It could also be argued that 0-back is not a level of an n-back task as no WM items are stored, and so the behavioural responses to this condition may not follow the same trends as other n-back levels. We also performed the same analysis with the residual PTRs after regressing out the contribution of OTRs. This allowed us to see if relationships between PTRs and RT were strengthened or weakened by the removal of any OTR contribution to signal modulations.

### 3. Results

#### 3.1. Behavioural Results

Analysis of button presses yielded the group-averaged behavioural results shown in Fig. 2, including targets hit (TH), false presses (FP) and reaction times (RT). All three behavioural metrics modulated significantly ( $p < 0.05$ , rm-ANOVA) with task condition. Post-hoc t-tests revealed that RT modulated significantly ( $p < 0.05$ , t-test) between all pairs of conditions, whereas TH and FP did not show a significant difference between 0-back and 1-back.

#### 3.2. Activation Maps

Investigation of the gamma band responses in both the task and PTR time-windows showed that there were no visible gamma (30 - 100 Hz) responses. A response which appeared in the low frequency gamma (30 - 50 Hz) band appeared to be bleed-through from the beta band. Therefore, no further analysis on the gamma band was conducted.

Pseudo T-statistic (T-stat) maps showing OTR modulations with condition can be seen in Fig. 3A, for the theta [4 - 8 Hz] (Fig. 3Ai), alpha [8 - 13 Hz] (Fig. 3Aii) and beta [13 - 30 Hz] (Fig. 3Aiii) bands. Additional contrasts of task (0.5 - 29.5 s) vs rest (30.5 - 59.5 s) can be seen in the Supplementary Information section (Fig. S5). In Fig. 3, positive values represent an increase in oscillatory power in the 2-back condition compared with the 0-back condition, while negative values represent a decrease in oscillatory power between these conditions. Fig. 3A shows that: power in the theta band increased in the prefrontal cortex and decreased in parietal and lateral visual regions; power in the alpha band decreased in parietal and lateral visual regions; power in the beta band decreased in the parietal lobe and to a lesser extent, the frontal eye fields, during the 2-back condition compared with the 0-back condition.

Fig. 3B shows T-stat maps of modulations in the theta (Fig. 3Bi), alpha (Fig. 3Bii) and beta (Fig. 3Biii) bands during the post-task (PTR) time-window. When comparing the 2-back with the 0-back condition, power in the theta band decreased in the prefrontal cortex, the right



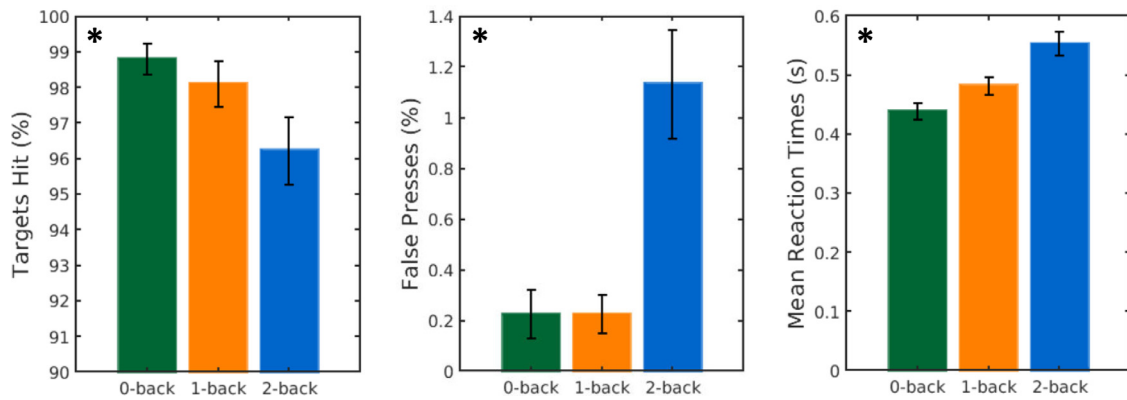


**Fig. 2.** Behavioural responses to the n-back task.

Behavioural results from the n-back task showing the modulation in targets hit (TH), false presses (FP) and reaction times (RT) with condition, averaged over all subjects. Error bars denote the standard error over subjects. Significant ( $p < 0.05$ , rm-ANOVA) modulation of measured response with condition is denoted by an asterisk (\*). Post-hoc t-tests revealed that RT modulated significantly ( $p < 0.05$ , t-test) between all pairs of conditions, but TH and FP did not modulate significantly between 0-back and 1-back.

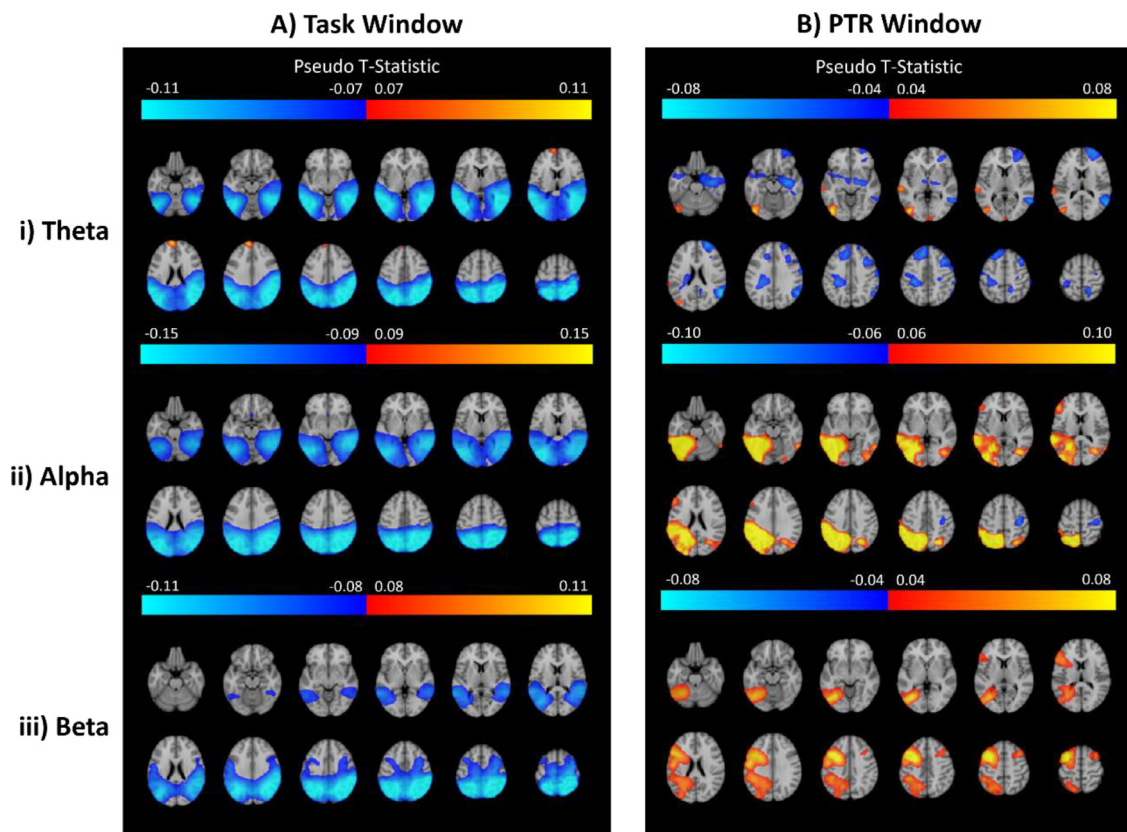


**Fig. 3.** Group T-stat maps.

A set of group pseudo T-statistic (F-stat) maps, displayed on MNI-152 brain, found by contrasting the 2-back condition with 0-back, during the task window (column A, 0.5 - 29.5 s) and the PTR window (column B, 31.5 - 33.5 s). Results are filtered into the theta (row i, 4 - 8 Hz), alpha (row ii, 8 - 13 Hz) and beta (row iii, 13 - 30 Hz) bands. Panels Ai and Aii mirror previous studies, showing a frontal theta event-related synchronisation (ERS), and posterior theta and alpha event-related desynchronisation (ERD). Panel Aiii shows a beta ERD in the dorsal attention network (DAN), while panels Bii and Biii show alpha and beta ERS in the left lateralised DAN in the PTR window.

temporoparietal junction (TPJ), and the left motor cortex, whilst it increased in the left lateral visual and left auditory cortices (Fig. 3Bi). Power in the alpha band increased in the left parietal and left lateral visual regions (Fig. 3Bii). Power in the beta band increased in the left frontal eye field and left parietal cortex, and to a lesser extent, the right frontal eye field (Fig. 3Biii). These observations enabled the selection of regions for further interrogation shown in Table 1.

### 3.3. Peak Timecourses

Visual inspection of group F-stat maps in Fig. 3 allowed identification of relevant brain regions activated by the task. The anatomical masks shown in Table 1 were then used to interrogate the strongest responses over the group (Przedzick et al. 2013; Wilson et al. 2015; Mars et al. 2012; Tzourio-Mazoyer et al. 2002).

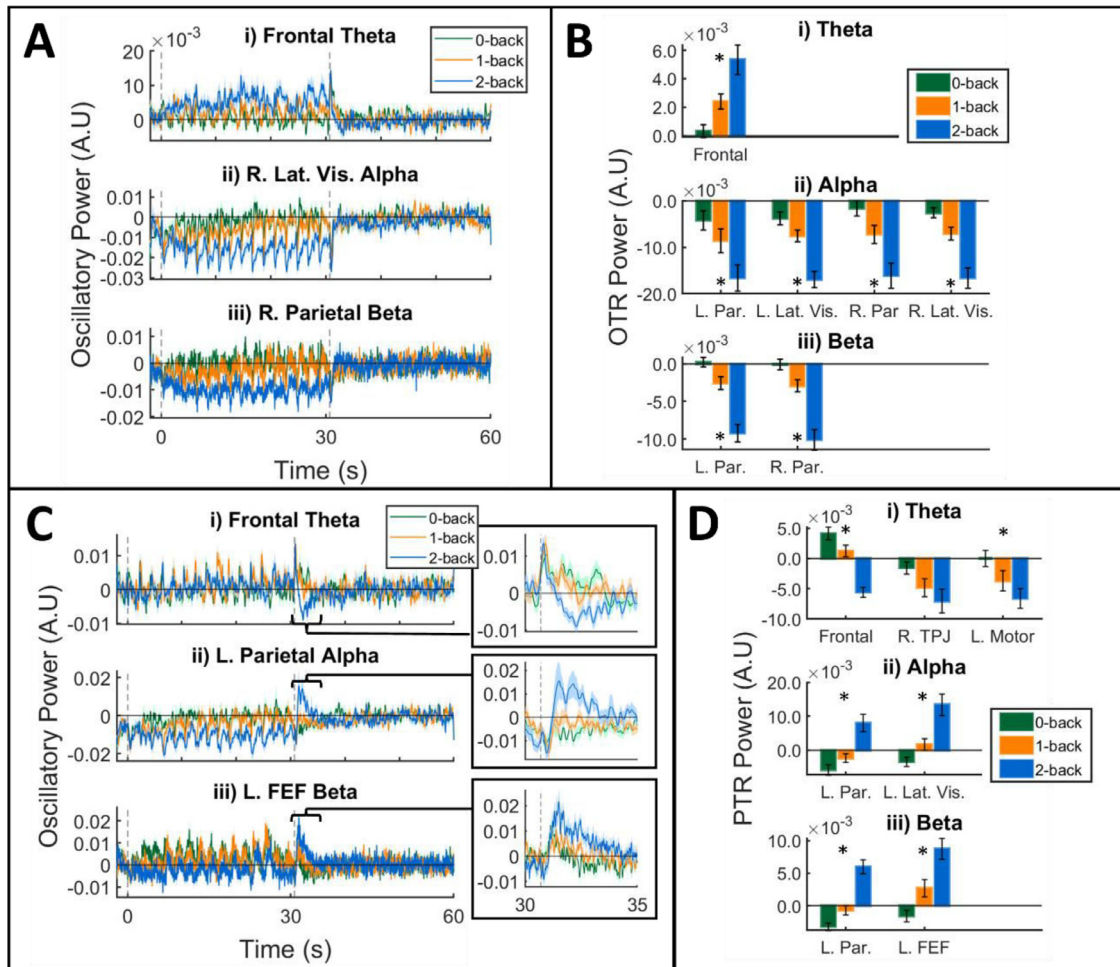


**Fig. 4.** Group timecourses and average power modulations.

Timecourses and bar charts from peak T-stat locations in each frequency band. Panels A and C show group averaged timecourses from representative OTR and PTR locations in each frequency band (other timecourses can be seen in Fig. S1 and S3). Timecourses were averaged during the relevant time windows to give the average power over the time windows for each region which is displayed in the bar charts (panels B [OTR] and D [PTR]). Panels A and B show effects during the OTR window (0.5 - 29.5 s), whilst panels C and D show effects during the PTR window (31.5 - 33.5 s). Bar charts that show significant ( $p < 0.05$ , rm-ANOVA) change across conditions are marked with an asterisk (\*). Shading around timecourses (A and C) and error bars (B and D) denote standard error over subjects for each measure.

As can be seen in Table 1, parietal and lateral visual theta responses were excluded from the rest of the analysis because time-frequency spectrograms (TFS) revealed that the effects were likely bleed-through from the alpha band. The frontal eye field beta OTR responses were also excluded as they were relatively weak compared to those in the parietal lobe (Fig. 3 row iii).

Fig. 4A shows representative group timecourses from peak OTR locations in each frequency band (all region timecourses are shown in Fig. S1). The timecourses show a large change in OTR power in each of the frequency bands in 2-back compared with the other conditions. The time-averaged OTR for all regions-of-interest, depicted in Table 1, can be seen in Fig. 4B. The TFS for each of these regions for the 2-back condition can also be seen in Figure S2. When averaging over the OTR time window, all regions interrogated modulated significantly ( $p < 0.05$ , rm-ANOVA) with task condition after Bonferroni correction, as shown in Fig. 4B. Post-hoc t-tests showed that for all regions, there were significant ( $p < 0.05$ , t-test) modulations between all pairs of conditions. Interestingly, the change in oscillatory power between 2-back and 1-back was much larger in magnitude than the change between 1-back and 0-back.

Fig. 4C shows representative group timecourses from peak PTR locations in each frequency band, with the inset highlighting the time-

courses during the PTR time-window (all region timecourses are shown in Fig. S3). Post-task rebounds in the alpha (Fig. 4Cii) and beta bands (Fig. 4Ciii), previously only observed in the primary cortex following movement or visual stimuli, are clearly visible in the left parietal cortex and left frontal eye field, both regions which are associated with higher cognitive activity. The theta band (Fig. 4Ci) also shows a clear PTR, although this is an event-related desynchronisation (ERD) rather than an event-related synchronisation (ERS) and is primarily seen in the 2-back condition. The TFS for each of these regions for the 2-back condition can also be seen in Figure S4.

Fig. 4D shows the average PTR amplitude in all the regions of interest named in Table 1. Apart from theta in the right TPJ, all PTRs modulated significantly ( $p < 0.05$ , rm-ANOVA) with task condition after Bonferroni correction. As found for the task region responses, post-hoc t-tests showed that for alpha band activity in left lateral visual and beta band activity in left parietal regions and left frontal eye field, there were significant modulations in the PTRs between all pairs of conditions. However, in contrast to the task-window responses, the PTRs in the theta band activity in frontal and left motor regions and alpha band activity in the left parietal region, there were no significant differences between the 0-back and 1-back conditions, with 2-back condition driving the measured PTR modulations in these regions.

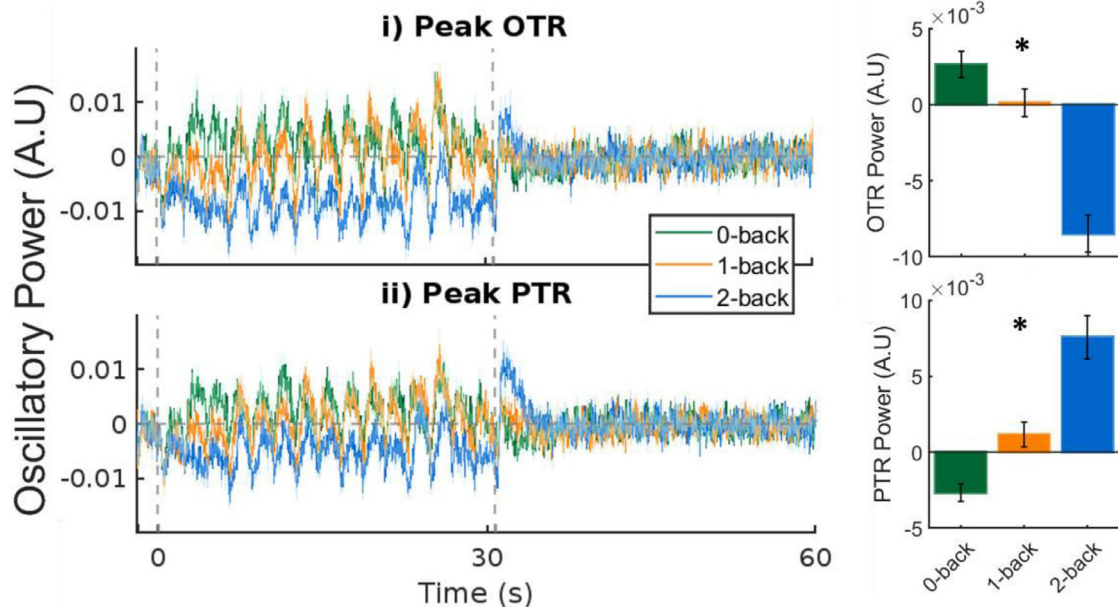


Fig. 5. Dorsal attention network.

Group-averaged beta timecourses across the whole dorsal attention network (DAN), at locations of peak activity during the OTR (i, 0.5 - 29.5 s) and PTR (ii, 31.5 - 33.5 s) time-windows. Bar charts on the right show average power in the corresponding time windows across conditions. Activity during both time windows modulated significantly ( $p < 0.05$ , rm-ANOVA) with task condition, denoted with an asterisk (\*). Post-hoc t-tests showed that all pairs of conditions varied significantly ( $p < 0.05$ , t-test) in both time-windows. Shading around timecourses and error bars on bar charts represent standard error over subjects for each measure.

### 3.4. Dorsal Attention Network

In both time-windows, beta band activity was localised to the dorsal attention network (DAN). The group-averaged timecourse for beta activity averaged over all nodes of the DAN can be seen in Fig. 5, with maximum OTR modulation shown in Fig. 5i and maximum PTR modulation shown in Fig. 5ii. Both the OTR in Fig. 5i and the PTR in Fig. 5ii modulated significantly ( $p < 0.05$ , rm-ANOVA) between all pairs of conditions.

### 3.5. Motor Cortex Response

Fig. 6 shows the group-average peak motor response in the beta band when contrasting the PMBR to the MRBD. The peak PMBR location is shown in the T-stat map in Fig. 6A, found by contrasting the PMBR window (0.5 - 1.5 s following each button press) with the MRBD window (-0.5 - 0.5 s around each button press). The group-average timecourse in response to correct button presses is shown in Fig. 6B for each condition, with the button press occurring at  $t = 0$ . The baseline used (48 - 58 s) was the same as the timecourses in Figs. 4, S1 and S3. Using rm-ANOVA, we found no significant modulation between task condition in either the MRBD or PMBR. SLR results are shown in Fig. 6C, comparing average PMBR following button presses with average PTR in the DAN following task blocks, for each subject. PMBR correlated significantly with PTR in the DAN, despite the PMBR not modulating with task condition, showing that subjects with large PMBRs tend to also have large PTRs in the DAN. However, the two responses differ in that the DAN is functionally modulated by the n-back task, whereas the PMBR is not.

### 3.6. OTR-PTR Relationship

The residual PTR amplitudes after regressing out OTR amplitudes can be seen in Fig. 7. In all regions where both OTR and PTR effects were observed, the residual PTR signals still showed significant modulation between conditions (Bonferroni corrected), suggesting that the OTR and PTR are largely independent. In addition, the time locked oscillatory

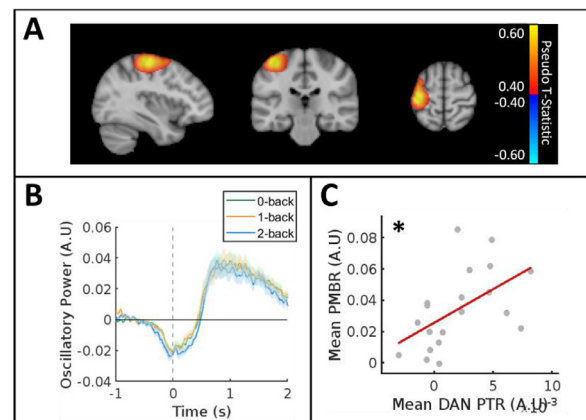


Fig. 6. Post-movement beta rebound.

The well-studied beta response to movement in the motor cortex. Panel A shows a T-stat map found by contrasting the PMBR period (0.5 - 1.5 s relative to button press) with the MRBD period (-0.5 - 0.5 s relative to button press) across all conditions. A clear positive peak can be seen in the left (contralateral) motor cortex. Panel B shows the extracted timecourses for each condition, averaged over all correct button presses and over all subjects. The time axis is set such that zero is the time of the button press. The shaded area around each line denoting the standard error over subjects. There were no significant modulations between conditions during the MRBD nor the PMBR. Baselines were removed from timecourses using 48 - 58 s used in Figs. 4, S1 and S3. Panel C shows the relationship over subjects between the mean PMBR with the mean DAN PTR over all conditions. \* denotes a significant ( $p < 0.05$ ) correlation.

responses following each stimulus presentation are not related to the PTR - this is explored in the Supplementary Information (Figure S6).

### 3.7. Neural-Behaviour Correlations

The results of relating RT to oscillatory activity are shown in Fig. 8, with OTR against RT in Fig. 8A and PTR against RT in Fig. 8B. The anal-



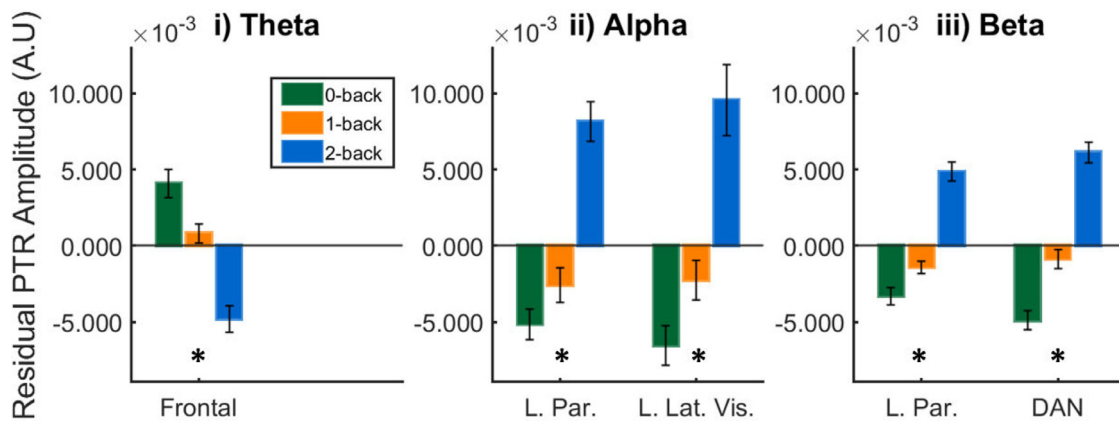


Fig. 7. Residual PTR power modulations.

Average PTR power (as shown in Fig. 4) after the OTR signals have been regressed out for each subject. Only the regions and frequency bands where both an OTR and PTR modulation were measured were included in these analyses. A significant ( $p < 0.05$ , RM-ANOVA) change across conditions is marked with an asterisk (\*). Error bars denote standard error over subjects.

ysis showed no significant correlation between oscillatory power in the task window (0.5 – 29.5 s) and RT, for any of the regions. However, the alpha band PTR amplitude in the left lateral visual region showed a significant ( $p < 0.05$ , SLR) positive correlation with RT, meaning that a subject with greater increase in alpha PTR amplitude also had longer RT in 2-back compared to 1-back condition. Similar correlation was seen for left parietal alpha power and RT, albeit a trend ( $p < 0.1$ , SLR). These results were not corrected for multiple comparisons, as with only 20 participants, methods such as Bonferroni correction would likely suppress any real effects in the data.

Residual PTRs in the same four regions were correlated with RT, as shown in Fig. 8C. The left lateral visual alpha band PTR and RT correlation remained the same, however there was no longer a trend between left parietal alpha band PTR and RT. Interestingly, the frontal theta band relationship with the RT became significant. In this region a large change theta ERD in the PTR window was associated with a small change in RT between the two conditions.

#### 4. Discussion

Post-task responses have been studied extensively in the motor cortex (Barratt et al. 2017; Gascoyne et al. 2021; Hunt et al. 2019; Liddle et al. 2016; Fry et al. 2016; Pakenham et al. 2020; Gaetz et al. 2020; Jurkiewicz et al. 2006), especially in the beta band. However, despite several standing hypotheses, there is no clear consensus on the functional role of PMBRs, and there has been no evidence that PTRs occur outside of the primary cortex following complex cognitive processes. We showed that PTRs are a ubiquitous phenomenon, measured in regions across the brain, including higher cognitive regions associated with the dorsal attention network (DAN), and across the theta, alpha, and beta frequency bands. These PTRs follow cessation of higher cognitive processes (attention, working memory) rather than simple sensory processes such as movement or visual stimulation. In several regions, the PTR magnitudes increased significantly with WM load, suggesting a functional relationship to cognitive scaling. Furthermore, we show that PTRs contain unique information through several analyses. First, they are not simply explained by the preceding OTRs (Fig. 7) or OSRs (Fig S6). In addition, the RT of a subject performing the task were predictive of alpha PTR amplitudes in lateral visual ( $p < 0.05$ , SLR) and parietal ( $p < 0.1$ , SLR) regions, whereas RT were not predictive of OTR amplitude in the same regions. When OTR amplitude was regressed from the PTR amplitude, the significant ( $p < 0.05$ , SLR) alpha correlation with RT remained and a significant ( $p < 0.05$ , SLR)

correlation between theta band PTR in frontal regions and RT was also revealed (Fig. 8).

Previous fMRI studies have found activations to an n-back task in the DAN that increase with load (Weinberger et al. 1996; Callicott et al. 2003; Blokland et al. 2008; Owen et al. 2005). However, until now, there has been limited identification of this network in electrophysiology studies, particularly in association with oscillatory responses. Luckhoo et al noted that left fronto-parietal network connectivity was modulated in the 8 – 20 Hz frequency band during the task period, but not significantly (Luckhoo et al. 2012). Huang et al (Huang et al. 2019) showed there is a change in the alpha and beta bands which appear to overlap with the DAN, but there was considerable spatial blurring of the responses making it difficult to identify the regions recruited. Previous EEG and MEG studies have more often reported modulation of the default mode network (DMN) during the task period (Brookes et al. 2011; Popov et al. 2018), including frontal pole and bilateral parietal regions, which we also observe (Figure S5). Unlike these studies, we observe clear modulations of the DAN in the beta band in both the task and post-task periods, as well as alpha modulations in the DAN during the PTR window. The frontal nodes of the DAN are most pronounced in the positive beta modulations during the PTR period (Fig. 3Biii), but they can also be seen in the beta ERD during the task period (Fig. 3Aiii). The modulations in the parietal nodes of the DAN are most strongly seen in the alpha and beta bands during the task period (Fig. 3Aii, 3Aiii), as well as the alpha band during the PTR period (Fig. 3Bii). It is worth noting that during the task window the posterior nodes (parietal cortex) of the DAN are more pronounced in both the alpha and beta bands, while the frontal nodes display much weaker activations. This may be why in previous studies, which did not examine the PTR window, these parietal activations were associated with the DMN rather than the DAN.

Overall, we see a decrease in DAN beta power during the task, followed by an increase in beta power above baseline following task cessation. Both parts of the response modulate significantly ( $p < 0.05$ , rm-ANOVA) across conditions (Fig. 5) although the modulations are not implicitly correlated (Fig. 7). Interestingly, we did not see any PMBR modulation with WM load to the button presses following target presentation (Fig. 6). We hypothesise that this is because the motor cortex is not specifically recruited for working memory processes during the n-back task, instead being recruited for the button press motor action, which does not change in difficulty across conditions.

In general, we suggest there are parallels which can be drawn between the PTR in the DAN to the n-back task and the PMBR in the motor cortex for a motor task. In both instances a network, known to be



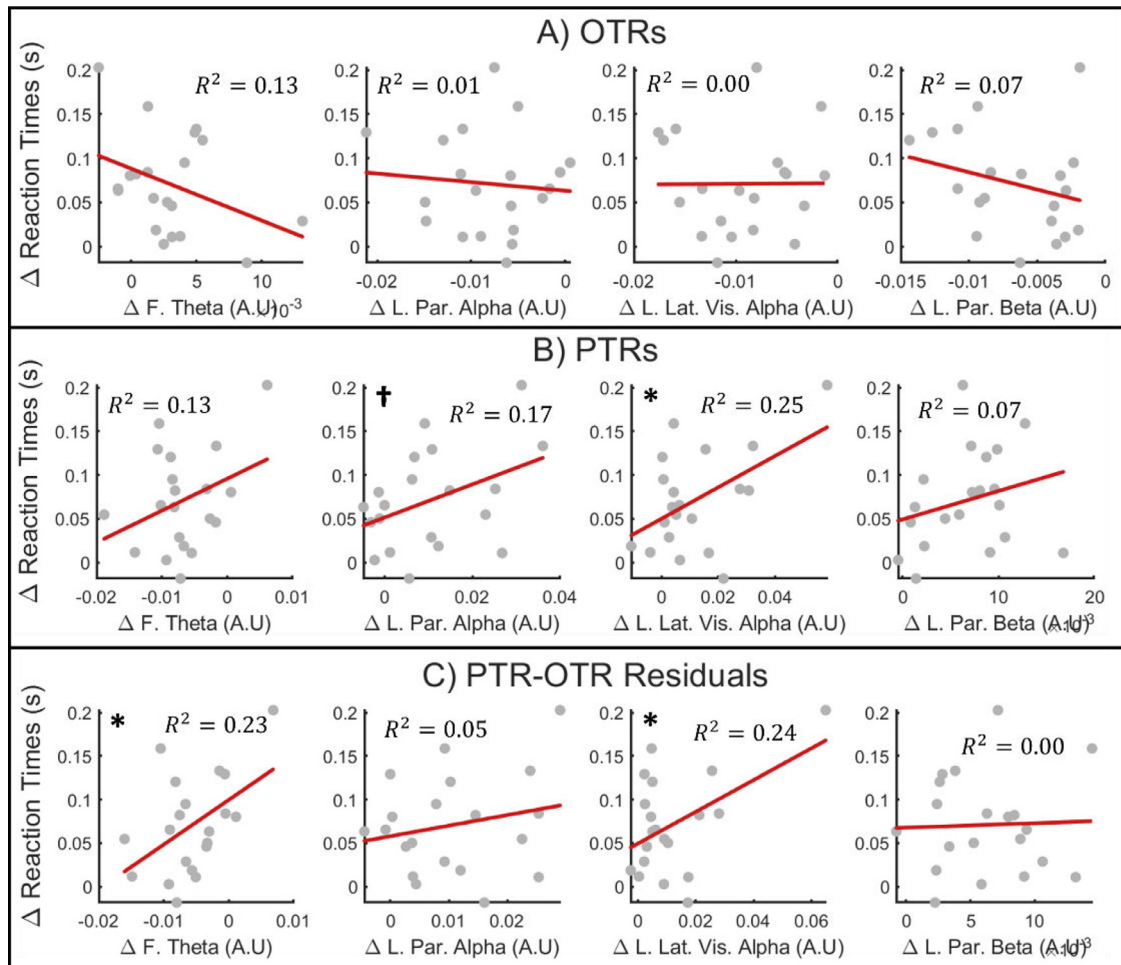


**Fig. 8.** Correlating reaction times to average oscillatory power.

Simple linear regressions across subjects between the change in reaction time ( $\Delta$ RT) and change in oscillatory power between 2-back and 1-back conditions, averaged over blocks. Panel A shows the OTR against RT, Panel B shows the PTR against RT and Panel C shows the PTR response after OTR response has been regressed out against RT. Only regions with T-stat peaks associated with both the OTR and PTR time windows were examined. An asterisk (\*) denotes a significant ( $p < 0.05$ ) relationship between measures; while a dagger (†) denotes a trend ( $p < 0.1$ ).  $R^2$  is the coefficient of determination denoting goodness of fit.

crucial for correct execution of the task, exhibits a beta ERD during the task, followed by a beta ERS after task cessation. Interestingly, we find a significant correlation between the average PMBR response and the average DAN PTR response over subjects (Fig. 6C), suggesting a link between these two responses, with subjects who exhibit a large PTR in the DAN also exhibiting a greater PMBR. However, it is difficult to determine whether this correlation is driven by a functional relationship between DAN PTRs and the PMBR or neural fingerprinting effects, i.e., some subjects have higher measured beta power which is reflected in both the DAN and motor cortex. We propose that the beta PTR is not unique to any particular task but is established in the cortical regions or networks most strongly engaged during the task. In the case of the n-back task, the networks which are modulated by task condition are those involved in higher cognitive processes, leading to PTR modulation in these regions. There is no change in the PMBR with task condition as the motor action (button press) remains the same, placing the same load on the motor network despite the changing WM load. Further work is needed to explore the links between responses in different regions to different tasks.

In addition to beta band PTRs, we also show responses in the alpha and theta frequency bands. Although alpha PTRs were visible in the DAN, there was a far stronger response in parietal than frontal regions. The alpha response was also seen in lateral visual regions during the task and PTR time-windows. The difference in the locations of the

responses may reflect the locations of the primary sources of alpha and beta, with both bands serving to transition these brain regions to rest. Increases in alpha are now synonymous with the concept of inhibiting task irrelevant information (Roux and Uhlhaas 2014; Klimesch et al. 2007; Sokoliuk et al. 2019; Jensen and Mazaheri 2010). Therefore, in the case of the PTR, the increase in alpha power that we observe most likely represents reduced attention to external stimuli to enable the brain to return to internal processes. Indeed, the idea that alpha and beta band activity are working in concert, and perhaps should not be distinguished, is a well-documented concept within the frameworks that explain the role of oscillations in WM tasks (Hanslmayr et al. 2016; Griffiths et al. 2019).

A novel observation that we report is a theta ERD following task cessation (Fig. 3Ai, 4Ci), mostly localised to the prefrontal cortex. We see several default mode network (DMN) regions modulate in the theta band, including the medial prefrontal cortex, inferior parietal lobules and temporoparietal junction (Fig. S5i). Other studies have also seen DMN regions activated in the theta band during an n-back task (Brookes et al. 2011; Luckhoo et al. 2012; Popov et al. 2018). Given the fMRI studies that show the DMN is suppressed during an n-back task (Pomarol-Clotet et al. 2008; Schneider et al. 2011), and the fact that theta power in DMN regions correlates negatively with BOLD (Meltzer et al. 2007), it is possible that the frontal theta ERD during the PTR window represents reactivation of a network that was suppressed during the task. Similar to alpha/beta PTRs in the DAN and visual net-

work, the theta ERD may act to re-establish resting network activity, but through re-activation rather than inhibition.

All PTR amplitudes in Fig. 8B increased with RT, regardless of sign of the PTR. The strongest relationships with RT were seen in the alpha band PTRs in left lateral visual ( $p < 0.05$ , SLR) and left parietal ( $p < 0.1$ , SLR) regions. Crucially, RT were not predictive of OTR amplitudes in the same regions (Fig. 8A). Removal of OTR contributions to the PTR amplitudes took away the trend between RT and left parietal alpha band, however the relationship remained in left lateral visual alpha band, and a new significant ( $p < 0.05$ , SLR) correlation was revealed between RT and residual PTR theta band activity in the frontal region (Fig. 8C). We did not correct these results for multiple comparisons, as with such a small number of participants, it is likely that this would lead to any real effects being suppressed. It is therefore important that these results are taken as a promising further indication that task and post-task oscillatory responses are driven by different aspects of cognition, rather than proof that PTRs are driven by reaction times. Our results corroborate the hypothesis posed by Pakenham *et al* that task difficulty modulates the PTR (Pakenham *et al.* 2020), however, we acknowledge that the findings presented require replication in larger cohorts in the future. The fact that the strongest relationships are seen in alpha band PTRs may reflect the unique role that alpha plays in suppressing responses to external stimuli in order to return to rest. It is also possible that we see the strongest relationship in alpha PTRs because this frequency band dominates the oscillatory response to an n-back task (Fig. S2, S4), i.e., the relevant frequency band may differ between tasks.

The lack of direct correlation between task performance metrics and OTRs is perhaps unsurprising given that the n-back task involves simultaneous encoding, retention and retrieval processes. In agreement with our findings, similar analysis using EEG showed no direct correlation between any single frequency band and behaviour (Popov *et al.* 2018). In an alternative approach, Takei *et al* separated the retention and encoding phases of the n-back task and showed that some alpha, beta and gamma oscillatory changes during the task were significantly related to hit rate and RT (Takei *et al.* 2016). A similar pattern was also observed by Huang *et al* (Huang *et al.* 2019), although we note that their behavioural-neuronal relationship is primarily driven by the mild traumatic brain injury patients and in the healthy controls there appears to be no clear correlation. Therefore, we suggest that the lack of correlation OTRs with behaviour is due to the brain performing multiple overlapping processes simultaneously, whereas in the PTR period the brain is performing a single unique function to inhibit external inputs and allow the brain to return to internal processing of the resting state. The level of inhibition required depends on cognitive demand felt by the participant, which is reflected in RT. Repetition of these tests with larger cohorts would confirm that there is no relationship between OTR and RT.

Future studies should use different modalities and paradigms to investigate the phenomena presented in this paper. Previous studies using concurrent EEG-fMRI have found that electrophysiological PTRs to median nerve and visual stimuli correspond to undershoots in BOLD data (Mullinger *et al.* 2017). The use of concurrent EEG-fMRI would allow us to directly explore the BOLD correlates of the PTRs presented in this paper. It would also facilitate the study of deep brain structures that are difficult to observe with EEG or MEG, providing a more complete picture of functional network dynamics when the brain moves between active and resting states. Future studies should also look at different patient populations to see if PTRs following higher cognitive processes are modulated by illness in the same way as the PMBR or if there are different mechanisms in play.

## 5. Conclusion

We used a bespoke n-back task to investigate PTRs in brain regions and networks associated with higher cognition. Our investigation revealed that PTRs are a ubiquitous phenomenon in the brain, occurring in

multiple frequency bands (theta, alpha, beta) and brain regions outside of the primary cortex, following cessation of higher cognitive processes. We believe we are the first to report post-task beta rebounds in the DAN, which modulate significantly ( $p < 0.05$ , rm-ANOVA) with WM load and may serve to inhibit network activity to return to rest. We also report negative theta PTRs which may represent re-activation of networks that were suppressed during the task. Alpha PTRs correlated with RT in left lateral visual ( $p < 0.05$ , SLR) and left parietal ( $p < 0.1$ , SLR) regions, while OTRs in the same region showed no correlation with RT – this result suggests that PTRs are a unique marker of brain function, although replication with larger cohorts is required to confirm this. Together our results suggest that PTRs in different frequency bands work in concert to re-establish resting brain activity, by means of inhibition or re-activation of functional networks. We provide evidence that PTRs may depend on task difficulty, such that greater cognitive demand in active networks requires PTRs of greater amplitude to return to rest.

## Data and Code Statement

All data and code can be made available upon request through a data sharing agreement with the authors.

## Declaration of Competing Interest

none.

## Credit authorship contribution statement

**Sebastian C. Coleman:** Conceptualization, Methodology, Software, Formal analysis, Investigation, Writing – original draft, Writing – review & editing, Visualization. **Zepekha A. Seedat:** Conceptualization, Software, Investigation, Writing – review & editing. **Anna C. Whittaker:** Methodology, Writing – review & editing. **Agatha Lenartowicz:** Conceptualization, Writing – review & editing. **Karen J. Mullinger:** Conceptualization, Methodology, Formal analysis, Writing – original draft, Writing – review & editing, Supervision.

## Data Availability

Data will be made available on request.

## Acknowledgements

We thank the SPMIC for providing funds to cover the scanning for this project and the University of Nottingham for funding SCC's PhD. We thank Matthew Brookes and Stephen Mayhew for useful conversations throughout this project.

## Supplementary materials

Supplementary material associated with this article can be found, in the online version, at doi:[10.1016/j.neuroimage.2022.119801](https://doi.org/10.1016/j.neuroimage.2022.119801).

## References

- Babiloni, C., Brancucci, A., Capotosto, P., Romani, G.L., Arendt-Nielsen, L., Chen, A.C., Rossini, P.M., 2005. Slow cortical potential shifts preceding sensorimotor interactions. *Brain Res Bull* 65, 309–316.
- Barratt, E.L., Tewarie, P.K., Clarke, M.A., Hall, E.L., Gowland, P.A., Morris, P.G., Francis, S.T., Evangelou, N., Brookes, M.J., 2017. Abnormal task driven neural oscillations in multiple sclerosis: A visuomotor MEG study. *Hum Brain Mapp* 38, 2441–2453.
- Blokland, G.A., McMahon, K.L., Hoffman, J., Zhu, G., Meredith, M., Martin, N.G., Thompson, P.M., de Zubicaray, G.I., Wright, M.J., 2008. Quantifying the heritability of task-related brain activation and performance during the N-back working memory task: a twin fMRI study. *Biol Psychol* 79, 70–79.
- Brookes, M.J., Wood, J.R., Stevenson, C.M., Zumer, J.M., White, T.P., Liddle, P.F., Morris, P.G., 2011. Changes in brain network activity during working memory tasks: a magnetoencephalography study. *Neuroimage* 55, 1804–1815.

- Callicott, J.H., Egan, M.F., Mattay, V.S., Bertolino, A., Bone, A.D., Verchinski, B., Weinberger, D.R., 2003. Abnormal fMRI response of the dorsolateral prefrontal cortex in cognitively intact siblings of patients with schizophrenia. *Am J Psychiatry* 160, 709–719.
- Chen, R., Corwell, B., Hallett, M., 1999. Modulation of motor cortex excitability by median nerve and digit stimulation. *Exp Brain Res* 129, 77–86.
- Falkenstein, M., Hohnsbein, J., Hoormann, J., Blanke, L., 1991. Effects of crossmodal divided attention on late ERP components. II. Error processing in choice reaction tasks. *Electroencephalogr Clin Neurophysiol* 78, 447–455.
- Frahm, J., Kruger, G., Merboldt, K.D., Kleinschmidt, A., 1996. Dynamic uncoupling and recoupling of perfusion and oxidative metabolism during focal brain activation in man. *Magn Reson Med* 35, 143–148.
- Fry, A., Mullinger, K.J., O'Neill, G.C., Barratt, E.L., Morris, P.G., Bauer, M., Folland, J.P., Brookes, M.J., 2016. Modulation of post-movement beta rebound by contraction force and rate of force development. *Hum Brain Mapp* 37, 2493–2511.
- Gaetz, W., Rhodes, E., Bloy, L., Blaskey, L., Jackel, C.R., Brodtkin, E.S., Waldman, A., Embick, D., Hall, S., Roberts, T.P.L., 2020. Evaluating motor cortical oscillations and age-related change in autism spectrum disorder. *Neuroimage* 207, 116349.
- Gascoyne, L.E., Brookes, M.J., Rathniah, M., Katshu, M., Koelewijn, L., Williams, G., Kumar, J., Walters, J.T.R., Seedat, Z.A., Palaniyappan, L., Deakin, J.F.W., Singh, K.D., Liddle, P.F., Morris, P.G., 2021. Motor-related oscillatory activity in schizophrenia according to phase of illness and clinical symptom severity. *Neuroimage Clin* 29, 102524.
- Gehring, W.J., Coles, M.G., Meyer, D.E., Donchin, E., 1995. A brain potential manifestation of error-related processing. *Electroencephalogr Clin Neurophysiol Suppl* 44, 261–272.
- Gehring, W.J., Goss, B., Coles, M.G.H., Meyer, D.E., Donchin, E., 2018. The Error-Related Negativity. *Perspect Psychol Sci* 13, 200–204.
- Gonzalez-Castillo, J., Saad, Z.S., Handwerker, D.A., Inati, S.J., Brenowitz, N., Bandettini, P.A., 2012. Whole-brain, time-locked activation with simple tasks revealed using massive averaging and model-free analysis. *Proc Natl Acad Sci U S A* 109, 5487–5492.
- Griffiths, B.J., Parish, G., Roux, F., Michelmann, S., van der Plas, M., Kolibius, L.D., Chelvarajah, R., Rollings, D.T., Sawlani, V., Hamer, H., Gollwitzer, S., Kreiselmeier, G., Staesina, B., Wimber, M., Hanslmayr, S., 2019. Directional coupling of slow and fast hippocampal gamma with neocortical alpha/beta oscillations in human episodic memory. *Proc Natl Acad Sci U S A* 116, 21834–21842.
- Hanlon, F.M., Shaff, N.A., Dodd, A.B., Ling, J.M., Bustillo, J.R., Abbott, C.C., Stromberg, S.F., Abrams, S., Lin, D.S., Mayer, A.R., 2016. Hemodynamic response function abnormalities in schizophrenia during a multisensory detection task. *Hum Brain Mapp* 37, 745–755.
- Hanslmayr, S., Staesina, B.P., Bowman, H., 2016. Oscillations and Episodic Memory: Addressing the Synchronization/Desynchronization Conundrum. *Trends Neurosci* 39, 16–25.
- Huang, M.X., Nichols, S., Robb-Swan, A., Angeles-Quinto, A., Harrington, D.L., Drake, A., Huang, C.W., Song, T., Diwakar, M., Risbrough, V.B., Matthews, S., Clifford, R., Cheng, C.K., Huang, J.W., Sinha, A., Yurgil, K.A., Ji, Z., Lerman, I., Lee, R.R., Baker, D.G., 2019. MEG Working Memory N-Back Task Reveals Functional Deficits in Combat-Related Mild Traumatic Brain Injury. *Cereb Cortex* 29, 1953–1968.
- Hunt, B.A.E., Liddle, E.B., Gascoyne, L.E., Magazzini, L., Routley, B.C., Singh, K.D., Morris, P.G., Brookes, M.J., Liddle, P.F., 2019. Attenuated Post-Movement Beta Rebound Associated With Schizotypal Features in Healthy People. *Schizophr Bull* 45, 883–891.
- Jensen, O., Gelfand, J., Kounios, J., Lisman, J.E., 2002. Oscillations in the alpha band (9–12 Hz) increase with memory load during retention in a short-term memory task. *Cereb Cortex* 12, 877–882.
- Jensen, O., Mazaheri, A., 2010. Shaping functional architecture by oscillatory alpha activity: gating by inhibition. *Front Hum Neurosci* 4, 186.
- Jurkiewicz, M.T., Gaetz, W.C., Bostan, A.C., Cheyne, D., 2006. Post-movement beta rebound is generated in motor cortex: evidence from neuromagnetic recordings. *Neuroimage* 32, 1281–1289.
- Klimesch, W., Sauseng, P., Hanslmayr, S., 2007. EEG alpha oscillations: the inhibition-timing hypothesis. *Brain Res Rev* 53, 63–88.
- Liddle, E.B., Price, D., Palaniyappan, L., Brookes, M.J., Robson, S.E., Hall, E.L., Morris, P.G., Liddle, P.F., 2016. Abnormal salience signaling in schizophrenia: The role of integrative beta oscillations. *Hum Brain Mapp* 37, 1361–1374.
- Luckhoo, H., Hale, J.R., Stokes, M.G., Nobre, A.C., Morris, P.G., Brookes, M.J., Woolrich, M.W., 2012. Inferring task-related networks using independent component analysis in magnetoencephalography. *Neuroimage* 62, 530–541.
- Mars, R.B., Sallet, J., Schuffelgen, U., Jbabdi, S., Toni, I., Rushworth, M.F., 2012. Connectivity-based subdivisions of the human right "temporoparietal junction area": evidence for different areas participating in different cortical networks. *Cereb Cortex* 22, 1894–1903.
- Meltzer, J.A., Negishi, M., Mayes, L.C., Constable, R.T., 2007. Individual differences in EEG theta and alpha dynamics during working memory correlate with fMRI responses across subjects. *Clin Neurophysiol* 118, 2419–2436.
- Mullinger, K.J., Cherukara, M.T., Buxton, R.B., Francis, S.T., Mayhew, S.D., 2017. Post-stimulus fMRI and EEG responses: Evidence for a neuronal origin hypothesised to be inhibitory. *Neuroimage* 157, 388–399.
- Owen, A.M., McMillan, K.M., Laird, A.R., Bullmore, E., 2005. N-back working memory paradigm: a meta-analysis of normative functional neuroimaging studies. *Hum Brain Mapp* 25, 46–59.
- Pakenham, D.O., Quinn, A.J., Fry, A., Francis, S.T., Woolrich, M.W., Brookes, M.J., Mullinger, K.J., 2020. Post-stimulus beta responses are modulated by task duration. *Neuroimage* 206, 116288.
- Pfurtscheller, G., 1981. Central beta rhythm during sensorimotor activities in man. *Electroencephalogr Clin Neurophysiol* 51, 253–264.
- Pfurtscheller, G., Lopes da Silva, F.H., 1999. Event-related EEG/MEG synchronization and desynchronization: basic principles. *Clin Neurophysiol* 110, 1842–1857.
- Pomarol-Clotet, E., Salvador, R., Sarro, S., Gomar, J., Vila, F., Martinez, A., Guerrero, A., Ortiz-Gil, J., Sans-Sansa, B., Capdevila, A., Cebamano, J.M., McKenna, P.J., 2008. Failure to deactivate in the prefrontal cortex in schizophrenia: dysfunction of the default mode network? *Psychol Med* 38, 1185–1193.
- Popov, T., Popova, P., Harkotte, M., Awiszus, B., Rockstroh, B., Miller, G.A., 2018. Cross-frequency interactions between frontal theta and posterior alpha control mechanisms foster working memory. *Neuroimage* 181, 728–733.
- Przedzicki, I., Izabela, Bagshaw, Andrew P., Mayhew, Stephen D., 2013. Some brains are more strongly functionally connected than others: a resting-state fMRI study of inter and intra network coherence. *Proc ISMRM* 603–610.
- Robson, S.E., Brookes, M.J., Hall, E.L., Palaniyappan, L., Kumar, J., Skelton, M., Christodoulou, N.G., Qureshi, A., Jan, F., Katshu, M.Z., Liddle, E.B., Liddle, P.F., Morris, P.G., 2016. Abnormal visuomotor processing in schizophrenia. *Neuroimage Clin* 12, 869–878.
- Roux, F., Uhlhaas, P.J., 2014. Working memory and neural oscillations: alpha-gamma versus theta-gamma codes for distinct WM information? *Trends Cogn Sci* 18, 16–25.
- Schneider, F.C., Royer, A., Grosselin, A., Pellet, J., Barral, F.G., Laurent, B., Brouillet, D., Lang, F., 2011. Modulation of the default mode network is task-dependent in chronic schizophrenia patients. *Schizophr Res* 125, 110–117.
- Sokolik, R., Mayhew, S.D., Aquino, K.M., Wilson, R., Brookes, M.J., Francis, S.T., Hanslmayr, S., Mullinger, K.J., 2019. Two Spatially Distinct Posterior Alpha Sources Fulfill Different Functional Roles in Attention. *J Neurosci* 39, 7183–7194.
- Takei, Y., Fujihara, K., Tagawa, M., Hironaga, N., Near, J., Kasagi, M., Takahashi, Y., Motegi, T., Suzuki, Y., Aoyama, Y., Sakurai, N., Yamaguchi, M., Tobimatsu, S., Ujita, K., Tsushima, Y., Narita, K., Fukuda, M., 2016. The inhibition/excitation ratio related to task-induced oscillatory modulations during a working memory task: A multimodal-imaging study using MEG and MRS. *Neuroimage* 128, 302–315.
- Tan, H., Jenkinson, N., Brown, P., 2014. Dynamic neural correlates of motor error monitoring and adaptation during trial-to-trial learning. *J Neurosci* 34, 5678–5688.
- Tuladhar, A.M., ter Huurne, N., Schoffelen, J.M., Maris, E., Oostenveld, R., Jensen, O., 2007. Parieto-occipital sources account for the increase in alpha activity with working memory load. *Hum Brain Mapp* 28, 785–792.
- Tzourio-Mazoyer, N., Landeau, B., Papathanassiou, D., Crivello, F., Etard, O., Delcroix, N., Mazoyer, B., Joliot, M., 2002. Automated anatomical labeling of activations in SPM using a macroscopic anatomical parcellation of the MNI MRI single-subject brain. *Neuroimage* 15, 273–289.
- Uludag, K., Blinder, P., 2018. Linking brain vascular physiology to hemodynamic response in ultra-high field MRI. *Neuroimage* 168, 279–295.
- van Zijl, P.C., Hua, J., Lu, H., 2012. The BOLD post-stimulus undershoot, one of the most debated issues in fMRI. *Neuroimage* 62, 1092–1102.
- Walter, W.G., 1968. The contingent negative variation: an electro-cortical sign of sensorimotor reflex association in man. *Prog Brain Res* 22, 364–377.
- Weinberger, D.R., Mattay, V., Callicott, J., Kotrla, K., Santha, A., van Gelderen, P., Duyn, J., Moonen, C., Frank, J., 1996. fMRI applications in schizophrenia research. *Neuroimage* 4, S118–S126.
- Wilson, R.S., Mayhew, S.D., Rollings, D.T., Goldstone, A., Przedzicki, I., Arvanitis, T.N., Bagshaw, A.P., 2015. Influence of epoch length on measurement of dynamic functional connectivity in wakefulness and behavioural validation in sleep. *Neuroimage* 112, 169–179.
- Yamamoto, D.J., Reynolds, J., Krmpotich, T., Banich, M.T., Thompson, L., Tanabe, J., 2014. Temporal profile of fronto-striatal-limbic activity during implicit decisions in drug dependence. *Drug Alcohol Depend* 136, 108–114.